Simulation study of the losses and influences of geminate and bimolecular recombination on the performances of bulk heterojunction organic solar cells*

Zhu Jian-Zhuo(朱键卓)†, Qi Ling-Hui(祁令辉), Du Hui-Jing(杜会静)‡, and Chai Ying-Chun(柴莺春)

College of Science, Yanshan University, Qinhuangdao 066004, *China*

(Received 6 March 2015; revised manuscript received 15 July 2015; published online 20 September 2015)

We use the method of device simulation to study the losses and influences of geminate and bimolecular recombinations on the performances and properties of the bulk heterojunction organic solar cells. We find that a fraction of electrons (holes) in the device are collected by anode (cathode). The direction of the corresponding current is opposite to the direction of photocurrent. And the current density increases with the bias increasing but decreases as bimolecular recombination (BR) or geminate recombination (GR) intensity increases. The maximum power, short circuit current, and fill factor display a stronger dependence on GR than on BR. While the influences of GR and BR on open circuit voltage are about the same. Our studies shed a new light on the loss mechanism and may provide a new way of improving the efficiency of bulk heterojunction organic solar cells.

Keywords: bulk heterojunction organic solar cells, losses, device simulation, geminate recombination, bimolecular recombination

PACS: 85.30.–z, 88.40.jr **DOI:** 10.1088/1674-1056/24/10/108501

1. Introduction

The bulk heterojunction (BHJ) organic solar cells (OSCs) have been intensively investigated in the past decade due to the advantages of being visibly transparent, compatible to flexible substrates, and light weight, etc.[1,2] Such devices can be fabricated via a low-cost and high throughput process, a promising new-energy technology.[3–6] The power conversion efficiencies (PCEs) of OSCs have reached over 10%,[7,8] and the performances of the OSCs can be improved by sophisticated modification over the properties of photoactive materials, morphological control of the organic films, and electrical contact for charge collection by the electrodes.[9–11]

The primary process of photocurrent generation is the generation of excitons after absorption of light. Then the excitons diffuse to the donor/acceptor interface and dissociate via ultrafast electron transfer into charge transfer (CT) states. In BHJ solar cells, the conversion of exciton-CT state has a quantum efficiency of almost unity. In order to generate a photocurrent, the bound CT states must dissociate into free electrons and holes and subsequently move to cathode and anode, respectively, before recombination processes take place. The loss and formation of CT states are believed to be key factors in determining the performances of the device. Two types of recombinations, i.e., the recombination of free carriers (non-geminate recombination) which forms CT states, and the recombination of CT states occurring at the donor/acceptor interface (geminate recombination), are closely related to the loss and formation of CT states. To understand the mechanisms behind the CT state process in BHJ solar cells, many researches of the two recombination processes have been performed.[12–15] However, there is hardly any joint and comparative research about the influences of geminate and bimolecular recombination on the performances of OSCs.

The bimolecular recombination (Langevin recombination) and trap-assisted recombination (SRH recombination) are two different types of non-geminate recombinations. In most of OSCs, especially in the OSCs with high efficiency, the traps are so few that the bimolecular recombination dominates the non-geminate recombination.[13,14] The influences of geminate recombination (GR) and bimolecular recombination (BR) on the performances of BHJ solar cells are studied in this article. And the losses in the OSCs are also studied. We find that a fraction of electrons (holes) in the device can be collected by anode (cathode). The direction of the corresponding current is opposite to the direction of photocurrent. This is another type of the CT state loss besides GR. The electrons (holes) collected by anode (cathode) are studied quantitatively for the first time. The performances of OSCs are improved largely if the electrons (holes) can be prevented from flowing out of the devices through anode (cathode).

*Project supported by the Natural Science Foundation of Hebei Province, China (Grant No. A2012203016), the Science Fund from the Education Department of Hebei Province, China (Grant Nos. QN20131103 and Z2009114), the Doctor Foundation of Yanshan University, China (Grant No. B580), and the Young Teachers' Research Project of Yanshan University, China (Grant No. 13LGB028).

†Corresponding author. E-mail: zhujz@ysu.edu.cn

‡Corresponding author. E-mail: hjdu@ysu.edu.cn

© 2015 Chinese Physical Society and IOP Publishing Ltd

Device simulation is an efficient way to study the interior working mechanism of OSCs.[16–19] Here, the studies are performed through the device simulation method. Many factors, such as mobility, morphology, etc., could affect the GR or/and BR rate.[17] Therefore OSCs with different GR or BR rates could be fabricated by employing different materials or different preparation technologies.[17] However besides different GR and BR rates, when employing different materials or different preparation technologies, other characteristics such as the dissociation rate of CT states, absorption spectrum of the devices, etc., can be changed, which may also influence the performances of the devices. Through the simulation method, one can obtain some results which cannot be obtained experimentally.[18]

2. Numerical model

The device is described by using the metal–insulator–metal picture. The BHJ layer is a mixture of donors and acceptors. It is considered as a homogeneous semiconductor. The energy difference between the lowest unoccupied molecular orbital (LUMO) of the acceptor and the highest occupied molecular orbital (HOMO) of the donor is considered to be an effective band gap ($E_{\rm gap}$) of the semiconductor. The thickness of the device is 100 nm. The rate of generation of CT states is assumed to be homogenous throughout the device. Though this is not to be strictly correct, it does not significantly influence the results and has been adopted by many researchers.[18–20]

We employ a one-dimensional drift-diffusion model to calculate the charge generation and transport in the device.[18–23] The electrostatic potential is calculated by Poisson equation

$$\frac{\partial^2}{\partial x^2}\Psi(x) = -\frac{q}{\varepsilon_0\varepsilon_{\rm r}}[p(x)-n(x)], \tag{1}$$

where x denotes the position within the device, q is the elementary charge, ε_0 is the vacuum dielectric constant, $\varepsilon_{\rm r}$ is the relative dielectric constant, relating the potential $\Psi(x)$ to the electron and hole densities $n(x)$ and $p(x)$, respectively. The charge carrier continuity equations are

$$\frac{\partial n(x)}{\partial t} = k_{\rm diss}(x)S(x) - R_{\rm B}(x) + \frac{1}{q}\frac{\partial J_{\rm n}(x)}{\partial x}, \tag{2}$$

$$\frac{\partial p(x)}{\partial t} = k_{\rm diss}(x)S(x) - R_{\rm B}(x) - \frac{1}{q}\frac{\partial J_{\rm p}(x)}{\partial x}, \tag{3}$$

where $J_{\rm n(p)}(x)$ is the electron (hole) current density, $R_{\rm B}(x)$ denotes the BR rate of electron and hole, and $k_{\rm diss}(x)S(x)$ represents the generation rate of electrons and holes [see Eq. (11)]. The relevant current equations are

$$J_{\rm n}(x) = -n(x)q\mu_{\rm n}\frac{\partial}{\partial x}\Psi(x) + qD_{\rm n}\frac{\partial}{\partial x}n(x), \tag{4}$$

$$J_{\rm p}(x) = -p(x)q\mu_{\rm p}\frac{\partial}{\partial x}\Psi(x) - qD_{\rm p}\frac{\partial}{\partial x}p(x), \tag{5}$$

$$D_{\rm n,p} = \frac{kT}{q}\mu_{\rm n,p}, \tag{6}$$

where $D_{\rm n}$ and $D_{\rm p}$ are the electron and hole diffusion coefficients respectively, $\mu_{\rm n}$ and $\mu_{\rm p}$ are the mobilities of electron and hole respectively, k is the Boltzmann's constant, and T is the absolute temperature. The cathode and anode are located at $x = 0$ and $x = L$ respectively, where L is the device thickness. One assumption is that the semiconductor is always in thermodynamic equilibrium at the contact interface. The work functions of cathode and anode are assumed to line up with the conduction band and the valence band of the semiconductor respectively and the two contacts are both therefore Ohmic. Using Boltzmann statistics

$$n(0) = N_{\rm C}, \tag{7}$$

$$n(L) = N_{\rm C}\exp\left(-\frac{E_{\rm gap}}{kT}\right), \tag{8}$$

$$p(0) = N_{\rm V}\exp\left(-\frac{E_{\rm gap}}{kT}\right), \tag{9}$$

$$p(L) = N_{\rm V}, \tag{10}$$

where $N_{\rm C(V)}$ is the effective density of states of conduction (valence) band. The CT state continuity equation is given by

$$\frac{{\rm d}S(x)}{{\rm d}t} = R_{\rm B}(x) - \alpha k_{\rm f}S(x) - k_{\rm diss}(x)S(x) + G_{\rm S}(x), \tag{11}$$

where $S(x)$ is the concentration of the CT states and α is the coefficient of GR strength, $\alpha k_{\rm f}$ is the decay rate at which the CT state decays to a ground state, $k_{\rm diss}(x)$ is the dissociation rate of the charge transfer states, and $G_{\rm S}(x)$ is the generation rate of the CT state. The dissociation rate of the CT states is described as

$$k_{\rm diss}(x) = \frac{3r_{\rm L}}{4\pi a^3}\exp\left(-\frac{E_{\rm B}}{kT}\right)\frac{{\rm J}_1(2\sqrt{-2b(x)})}{\sqrt{-2b(x)}}, \tag{12}$$

$$E_{\rm B} = \frac{q^2}{4\pi\varepsilon_{\rm r}\varepsilon_0 a}, \tag{13}$$

$$b(x) = \frac{q^3|F(x)|}{8\pi\varepsilon k^2T^2}, \tag{14}$$

where ${\rm J}_1$ is the Bessel function of order one, where $E_{\rm B}$ is the electron/hole pair binding energy, $F(x)$ is the field strength, and a is the electron/hole pair distance of a CT state. The pair distance is described by a normalized distribution function

$$f(r) = \frac{4}{\sqrt{\pi}a^3}r^2\exp\left(-\frac{r^2}{a^2}\right), \tag{15}$$

BR is expected to occur at the interface between the donor and acceptor in BHJ blends, with a rate

$$R_{\rm B}(x) = \beta r_{\rm L}[n(x)p(x) - n_{\rm i}^2], \tag{16}$$

$$r_{\rm L} = q\frac{\min(\mu_{\rm n},\mu_{\rm p})}{\varepsilon_0\varepsilon_{\rm r}}, \tag{17}$$

$$n_{\mathrm{i}} = \sqrt{N_{\mathrm{C}} N_{\mathrm{V}}} \exp\left(\frac{-E_{\mathrm{gap}}}{2kT}\right), \tag{18}$$

where β is the coefficient of BR strength. A device simulator ATLAS (Silvaco) is used for numerical simulations. All other parameters in the model used for computation are listed in Table 1.

Table 1. Overview of the parameters used in the simulations. According to Eq. (13), the bonding energy of CT states (E_{B}) is 0.236 eV.

Parameter	Symbol	Numerical value	Unit
Band gap	E_{gap}	1.0	eV
Electron mobility	μ_{n}	2.5×10^{-3}	$\mathrm{cm^2/V{\cdot}s}$
Hole mobility	μ_{p}	3×10^{-4}	$\mathrm{cm^2/V{\cdot}s}$
Efficient density of states	$N_{\mathrm{C}}, N_{\mathrm{V}}$	$2.5\times10^{19}, 2.5\times10^{19}$	$\mathrm{cm^{-3}}$
Generation rate	G_{S}	1.8×10^{21}	$\mathrm{cm^{-3}{\cdot}s^{-1}}$
Relative dielectric constant	ε_{r}	3.4	
e/h pair distance	a	1.8	nm
Decay rate	k_{f}	1.2×10^{6}	$\mathrm{s^{-1}}$

3. Results and discussion

The photovoltaic properties of the devices with different values of GR coefficient α and BR coefficient β are listed in Table 2 and the corresponding current density versus voltage (J–V) curves of these devices are shown in Figs. 1(a) and 1(b), respectively. According to Eq. (16), the BR intensity increases with β increasing. It is shown in Table 2 that as β increases, both the short circuit current density (J_{SC}) and open circuit voltage (V_{OC}) decrease. Experimentally, the BR intensity could be enhanced by various ways such as annealing which could increase the carrier mobility of the device.[17] However according to the work by Koster *et al.*, the annealing, which also influences the dissociation rate of the CT states, actually increases rather than reduces J_{SC}.[24]

Table 2. Solar cell characteristics.

α	β	$J_{\mathrm{SC}}/(\mathrm{A/m^2})$	V_{OC}/V	$W_{\mathrm{max}}/(\mathrm{W/m^2})$	FF
0.01		28.14	0.63	14.26	80.93%
0.1		28.05	0.62	13.75	79.65%
1	1	27.15	0.58	11.26	71.40%
2		26.21	0.57	9.81	66.04%
10		20.59	0.53	5.43	49.59%
50		10.12	0.50	1.92	38.20%
100		6.30	0.48	1.11	36.57%
	0.01	27.22	0.62	12.61	74.29%
	0.1	27.21	0.61	12.36	73.97%
	1	27.15	0.58	11.26	71.40%
1	2	27.10	0.57	10.68	69.57%
	10	26.73	0.53	8.88	62.68%
	50	25.48	0.49	6.78	54.27%
	100	24.54	0.47	5.90	50.84%

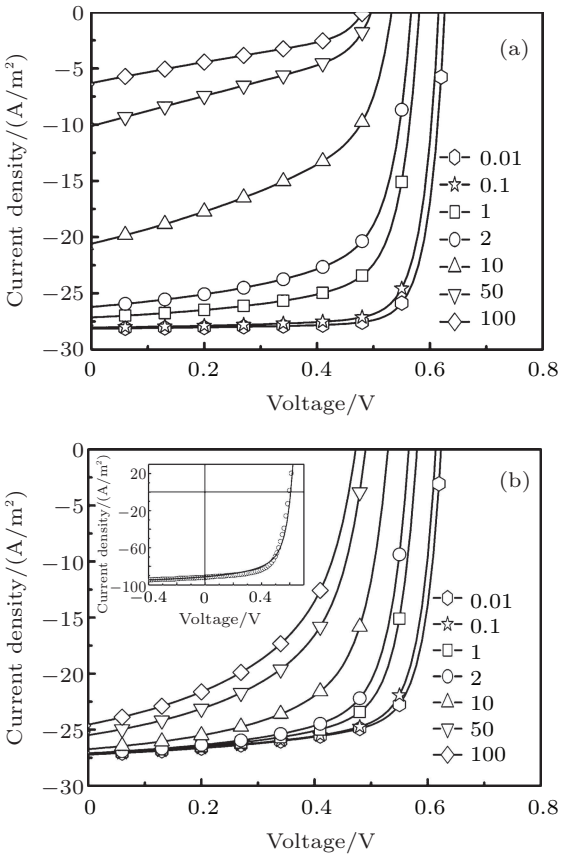


Fig. 1. Variations of current density with applied bias of devices with $\alpha = 0.01 \sim 100/\beta = 1$ (a) and $\alpha = 1/\beta = 0.01 \sim 100$ (b). Inset in panel (b): experimental (scatter, from Ref. [25]) and simulated (line) current density–voltage characteristics of the device under the stated conditions. Used parameters are: active layer thickness 97 nm, relative dielectric constant 3.4, hole mobility 1.5×10^{-4} $\mathrm{cm^2/V{\cdot}s}$, electron mobility 2.0×10^{-3} $\mathrm{cm^2/V{\cdot}s}$, band gap 1.0 eV, and efficient density of states 2.5×10^{19} $\mathrm{cm^{-3}}$. These parameters are the same as those in Ref. [25].

3.1. CT state losses in the OSC

Figure 2 shows the variations of BR and the GR rate with bias voltage when $\alpha = 1/\beta = 1$. And the inset displays the J–V characteristics. Both the BR rate and the GR rate increase with positive bias increasing. Especially at the voltage of W_{max}, the BR rate and GR rate both begin to increase rapidly. Figure 3 shows a schematic diagram of the electronic process in the OSCs under operation condition. Since the conversion of exciton-CT state has a quantum efficiency of almost unity, the ratio of the CT states contributing to the photocurrent determines the performances of the OSC. The more the CT state losses, the smaller the photocurrent is. According to Fig. 3, the GR describes a loss process of the CT states (call GR loss hereafter). The faster the GR occurs, the more slowly the free carriers are generated. So the increase of GR rate induces the photocurrent to decrease. The positive bias would impede the transport of electron and hole to the cathode and anode, respectively. So the BR probability of the free carriers increases with positive bias increasing. The BR of free carriers would increase the concentration of CT states. According to Eq. (11), the GR rate is proportional to the concentration

of the CT states, therefore the GR rate increases with positive voltage increasing.

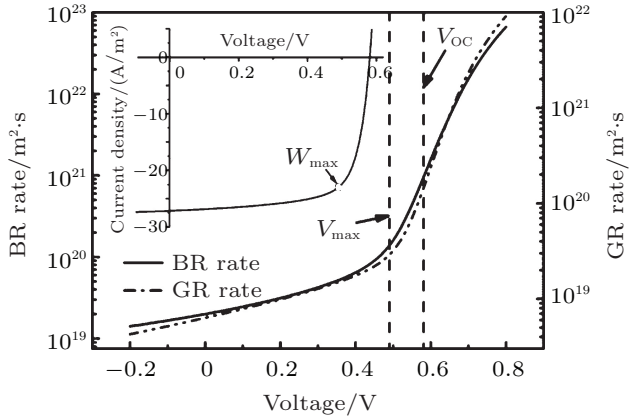


Fig. 2. Variations of BR rate and the GR rate per unit cross-sectional area in the device with bias voltage when $\alpha = 1/\beta = 1$. The BR rate and the GR rate here are the integrals of BR rate and the GR rate of different positions in the device from anode to cathode, respectively. The inset shows the J–V curve when $\alpha = 1/\beta = 1$.

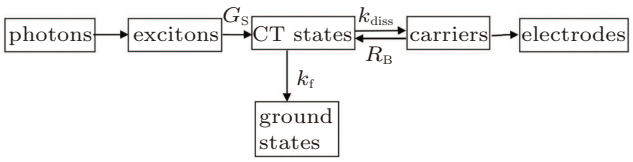


Fig. 3. Schematic diagram of the electronic process in BHJ solar cells under operation condition.

Figure 4 shows the hole and electron current densities in the device at different locations. Both the hole current at anode ($J_{H,ANODE}$) and the electron current at cathode ($J_{E,CATHODE}$) decrease as bias increases. When the bias is larger than V_{OC}, the $J_{H,ANODE}$ and $J_{E,CATHODE}$ become negative. This means that the electrons and holes are injected into the device from the cathode and anode, respectively. And the directions of the corresponding currents are opposite to the direction of photocurrent, while the values of electron current at anode ($J_{E,ANODE}$) and hole current at cathode ($J_{H,CATHODE}$) are negative in the entire bias range. This means that the electrons and holes from active layer flow out of the device at anode and cathodes, respectively. The directions of the $J_{E,ANODE}$ and $J_{H,CATHODE}$ are opposite to the photocurrent. Therefore the total current, which is the sum of electron and hole current and constant throughout the device, is smaller than $J_{H,ANODE}$ or $J_{E,CATHODE}$, (see Fig. 4(b), which shows that the photocurrent at a bias of 0.55 V is smaller than the corresponding $J_{H,ANODE}$), $J_{E,ANODE}$ and $J_{H,CATHODE}$ counteract parts of $J_{H,ANODE}$ and $J_{E,CATHODE}$, respectively. In other words, it is a form of CT state loss in OSCs (call current loss hereafter). This phenomenon has been observed by Koster *et al.*,[19] but has not been investigated quantitatively yet. Furthermore, the $J_{E,ANODE}$ and $J_{H,CATHODE}$ increase with the bias increasing [see Fig. 4]. Consequently, the current loss increases [see Fig. 6]. It is worth noting that if the current loss can be prevented, the performances of the device must be largely improved. Figure 5 shows the electron and hole concentration profile at open circuit when $\alpha = 1/\beta = 1$. The inset shows the corresponding energy levels. According to the energy levels, the electron should drift from the anode to cathode across the device. But the diffusion direction of the electrons is opposite to the drift direction due to the distribution of electron concentration in the device. In the vicinity of anode, the gradient of electron concentration is so large that the diffusion current of electrons is stronger than the drift current. Therefore the $J_{E,ANODE}$ is negative. The case of $J_{H,CATHODE}$ is similar.

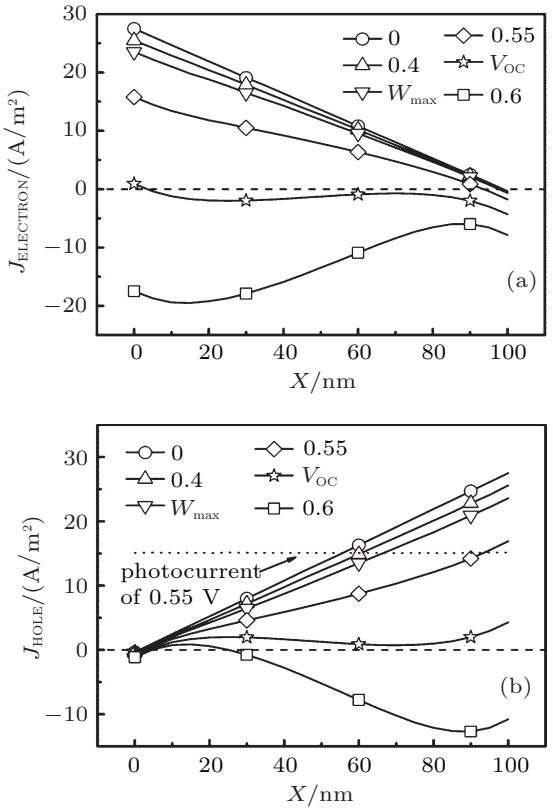


Fig. 4. Electron currents (a) and hole currents (b) at different positions of the device when $\alpha = 1/\beta = 1$ for various biases. The dashed line denotes the current density of 0 and the dotted line refers to the photocurrent when the bias is 0.55 V.

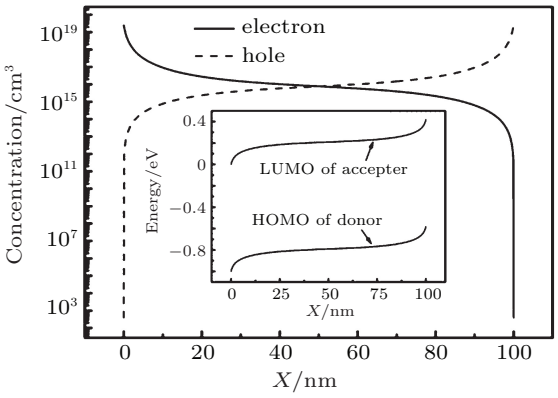


Fig. 5. Electron and hole concentrations at different positions in the device under open circuit conditions when $\alpha = 1/\beta = 1$. Inset: the corresponding energy levels.

Figure 6 shows the velocities of the electrons and holes flowing out of the device ($V_{\rm ELETRON}$, $V_{\rm HOLE}$), the velocity of the GR of CT states in the device ($V_{\rm GR}$), the velocity of CT state loss caused by current loss ($V_{\rm CL}$), and the velocity of the CT state generation in the device ($V_{\rm G}$) at different bias voltages. The values $V_{\rm ELETRON}$ and $V_{\rm HOLE}$ are equal. This is because the holes and electrons generate and recombine pairwise. According to Fig. 3, the photogenerated CT states vanish eventually by two ways: 1) relaxing to the ground through GR (GR loss); 2) flowing out of the device in the form of dissociated free electrons and holes ($J_{\rm E,CATHODE}$, $J_{\rm E,ANODE}$, $J_{\rm H,ANODE}$, and $J_{\rm H,CATHODE}$). Therefore, the sum of $V_{\rm GR}$ and $V_{\rm ELETRON}$ (or $V_{\rm HOLE}$) is equal to $V_{\rm G}$. This means that there are two and only two types of CT state losses: GR loss and current loss. Furthermore under the condition of open circuit, the $V_{\rm CL}$ is equal to $V_{\rm ELETRON}$ or $V_{\rm HOLE}$. This is because at $V_{\rm OC}$, the currents at anode and cathode are both 0. We can obtain $V_{\rm E,ANODE} = V_{\rm H,ANODE}$ and $V_{\rm E,CATHODE} = V_{\rm H,CATHODE}$ ($V_{\rm E,ANODE}$ represents the velocity of electron flowing out the device from the cathode. $V_{\rm H,ANODE}$, $V_{\rm E,CATHODE}$, and $V_{\rm H,CATHODE}$ are similar). We also have $V_{\rm CL} = V_{\rm H,CATHODE} + V_{\rm E,ANODE}$, $V_{\rm ELETRON} = V_{\rm E,ANODE} + V_{\rm E,CATHODE}$, and $V_{\rm HOLE} = V_{\rm H,ANODE} + V_{\rm H,CATHODE}$. Therefore, $V_{\rm CL} = V_{\rm ELETRON}$ and $V_{\rm CL} = V_{\rm HOLE}$ can be obtained.

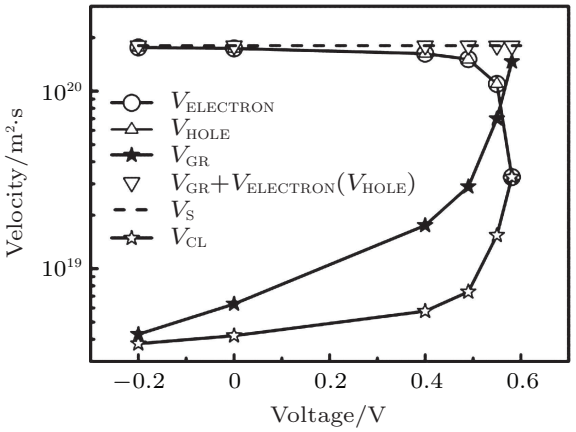


Fig. 6. $V_{\rm ELECTRON}$, $V_{\rm HOLE}$, $V_{\rm GR}$, $V_{\rm GR} + V_{\rm ELECTRON}$ (or $V_{\rm HOLE}$), $G_{\rm S}$, and $V_{\rm CL}$ as a function of bias voltage in the device with $\alpha = 1/\beta = 1$. All the values here are the integrals of the corresponding values of different positions in the device from anode to cathode.

3.2. Short circuit current

The values of $J_{\rm SC}$ respectively as a function of α and β are plotted in Fig. 7. The GR coefficient α has a stronger influence on the $J_{\rm SC}$ than β. The inset of Fig. 7 reveals the loss details of the CT state in the devices with different values of α and β respectively. With the increase of α or β, the current losses decrease while the GR losses increase. For the influence of α, when $\alpha < 0.6$ the current loss dominates. Though the enhancement of GR loss is fast, the changing of current loss is slow, so the variation of $J_{\rm SC}$ is small. When $\alpha > 0.6$ the GR loss dominates. The short circuit current decreases sharply, since the GR loss increases rapidly with α increasing. For the influence of β, the GR loss dominates in the entire range. For $\alpha = 100/\beta = 1$, the GR rate is about 21 times the value for the case of $\alpha = 1/\beta = 1$. While for $\alpha = 1/\beta = 100$, the GR rate is about 3.8 times the value in the case of $\alpha = 1/\beta = 1$. The GR loss influenced by α is larger than β, therefore α has a stronger influence on the $J_{\rm SC}$ than β.

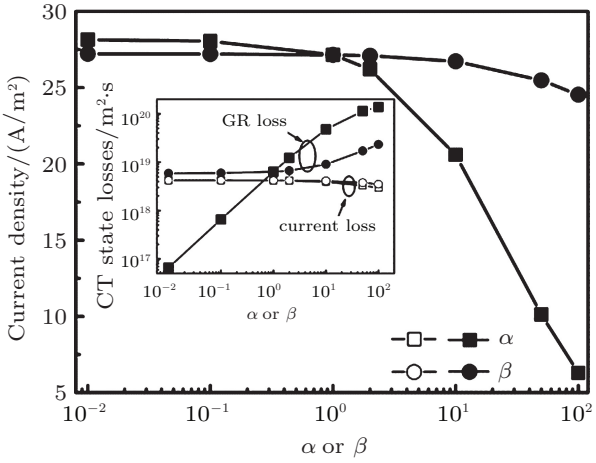


Fig. 7. Short circuit current densities for the devices with $\alpha = 0.01 \sim 100/\beta = 1$ or $\alpha = 1/\beta = 0.01 \sim 100$. Inset: the GR loss and current loss under short circuit conditions in the device with $\alpha = 0.01 \sim 100/\beta = 1$ or $\alpha = 1/\beta = 0.01 \sim 100$. The GR loss and current loss values here are the integrals of the corresponding values at different positions in the device from anode to cathode.

To investigate the GR loss influenced by α and β, we calculate the average dissociation ratio of bound CT states. The results are shown in Fig. 8. With the increase of α, the dissociation ratio decreases rapidly. While with the increase of β, the dissociation ratio almost remain unchanged or even increases slowly. Therefore GR loss influenced by α is larger than that by β.

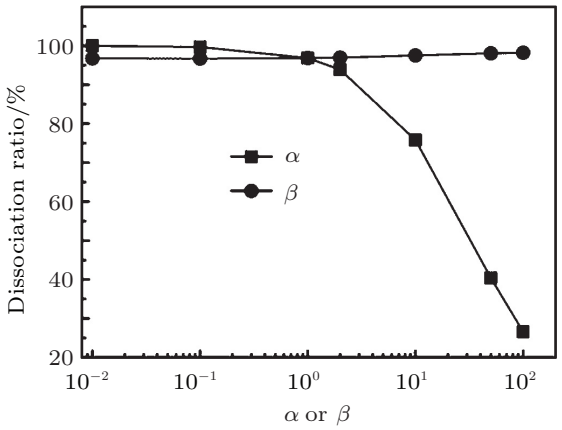


Fig. 8. Dissociation ratios of the CT states under short circuit conditions in the device with $\alpha = 0.01 \sim 100/\beta = 1$ or $\alpha = 1/\beta = 0.01 \sim 100$.

3.3. Open circuit voltage

The values of $V_{\rm OC}$ relatively as a function of α and β are plotted in Fig. 9. $V_{\rm OC}$ values decrease respectively with α and

β increasing. Moreover it is interesting that the V_{OC} values influenced by α and β are about the same. In Ref. [26], the V_{OC} obtained by authors is given by

$$V_{OC} = \frac{E_{gap}}{q} - \frac{kT}{q} \ln\left[\frac{(1-P)\gamma}{P}\frac{N_C N_V}{G_S}\right], \tag{19}$$

where γ is the BR constant and can be represented by βr_L, and P is the dissociation ratio of the CT states. The value of V_{OC} obtained by the formula is in good agreement with the corresponding experimental value. Using Eq. (18) one can further have

$$V_{OC} = \frac{E_{gap}}{q} - \frac{kT}{q} \ln\left(\frac{\alpha k_f \beta r_L}{k_{diss}}\frac{N_C N_V}{G_S}\right). \tag{20}$$

It is clear that α and β play the same role in the formula. Therefore the variations of V_{OC}, influenced by α and β, are almost the same. In Ref. [26] the relation of $V_{OC} \sim \ln(G_S)$ is linear. However the relations of $V_{OC} \sim \ln(\alpha)$ and $V_{OC} \sim \ln(\beta)$ are not linear here, especially when α or β is less than 1. That is because the dissociation rate of the CT state k_{diss} is field-dependent. When α or β changes, the concentration of charge carriers will change. According to Eq. (1) the electrostatic potential and electrical field will change with the concentration of charge carriers.

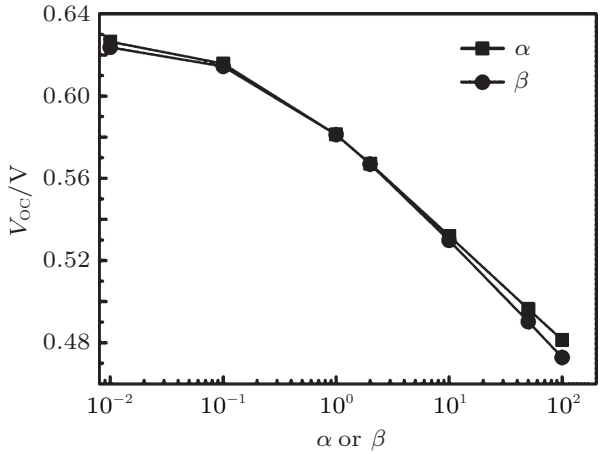


Fig. 9. Variations of V_{OC} values respectively with α and β of the devices with $\alpha = 0.01 \sim 100/\beta = 1$ or $\alpha = 1/\beta = 0.01 \sim 100$.

3.4. Fill factor

Figure 10 shows the fill factor (FF) values of the OSCs respectively as a function of α and β. The FF values decrease respectively with α and β increasing, and the influence of α is stronger than that of β. We consider the equivalent circuit of the OSC illustrated in the inset of Fig. 10. Both the larger series resistance (R_{sr}) and the smaller shunt resistance (R_{sh}) result in a lower FF.[27,28] As shown in Fig. 11, R_{sr} increases and R_{sh} decreases with α and β increasing. α influences R_{sh} more than β, but α influences R_{sr} less than β.

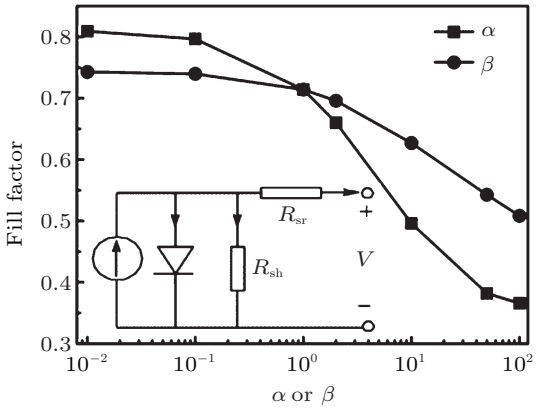


Fig. 10. Fill factor values of the devices with $\alpha = 0.01 \sim 100/\beta = 1$ or $\alpha = 1/\beta = 0.01 \sim 100$.

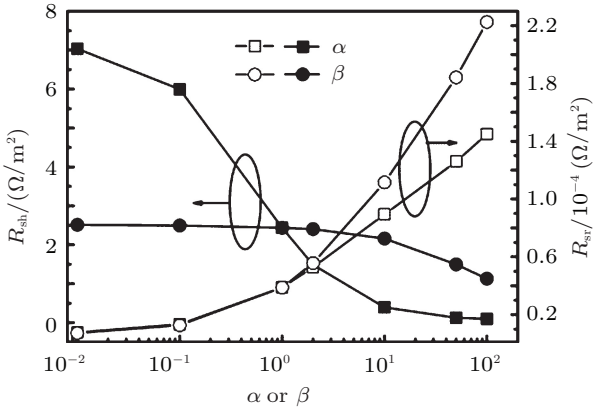


Fig. 11. Series resistance and shunt resistance of the devices with $\alpha = 0.01 \sim 100/\beta = 1$ or $\alpha = 1/\beta = 0.01 \sim 100$. The series resistances are calculated by the inverse slope of the J–V curve at roughly 0.2 V higher in bias than in open-circuit.[29] And shunt resistances are calculated by the inverse slope of the J–V curve at a reverse bias voltage of 1 V.[27]

R_{sr} induces a voltage drop on itself, it can separate the applied voltage from the diode. The larger the R_{sr}, the less the voltage drop on the diode is, which results in a slower increase of J with V rising, accordingly the less "square" the J–V curve becomes.[30,31] Generally R_{sr} is composed of (i) bulk resistance of the organic layer, (ii) bulk resistance of the electrodes, (iii) contact resistance of each interface in the device, and (iv) probe resistance. Since it is the numerical simulation here and the contacts of anode and cathode are Ohmic contacts, the resistances mentioned in items (ii)–(iv) are negligible.[28] The buildup of space charge should not play a role here. Space charges in BHJ solar cells are caused by a large difference in mobility between electrons and holes with a high illumination intensity.[32] While the mobility difference in this study is small (smaller than one order). If the space charge limited photocurrent plays a role, the FF should smaller than 42%.[32] Therefore the bulk resistance can be expressed as:[28]

$$R = \left(\frac{1}{nq\mu_n + pq\mu_p}\right)\frac{L}{A}. \tag{21}$$

Here, A is the cross-sectional area and L is the thickness of the device. We can see that the concentrations of hole and electrons determine the series resistance of the OSC. The hole and

electron concentration of the OSCs at open circuit are shown in Fig. 11. As α or β increases, the electron and hole concentrations both decrease, which is related to the increase of $R_{\rm sr}$. Moreover, the concentrations of electrons and holes are influenced more strongly by β than by α. Thus α influences $R_{\rm sr}$ less than β.

Shunt resistance represents the current leakage in the cells. It has the effect of separating the current in the equivalent circuit. Ideal $R_{\rm sh}$ should approach to infinity, so current flowing through $R_{\rm sh}$ is zero, i.e., there exists no current leakage in the device. The current will not change with the applied voltage at 0 or reverse bias. If $R_{\rm sh}$ is small, the current flowing through it cannot be neglected. The current will change with the applied voltage at 0 or reverse bias, which makes the J–V curve deviate from "square", thus leading to a lower FF. In the equivalent circuit, the shunt resistance under illumination ($R_{\rm sh}$) can be divided into two parts: one describes the shunt resistance in the dark ($R_{\rm shD}$), attributed to device pinholes and current leakage, and the other handles CT state dissociation ($R_{\rm shCT}$), and they are related by the following expression:[33]

$$\frac{1}{R_{\rm sh}} = \frac{1}{R_{\rm shD}} + \frac{1}{R_{\rm shCT}}. \tag{22}$$

According to the discussion in the previous sections, GR rate increases with α or β. And GR rate influenced by α is larger than by β. The larger the GR rate in the device, the smaller the $R_{\rm shCT}$ is, which results in a smaller $R_{\rm sh}$.

4. Conclusions

In this paper, we study the losses in the BHJ solar cells and the influences of BR and GR on the performances and properties of the devices through the method of device simulation. The current losses of CT states in BHJ solar cells, expressed as a fraction of electrons (holes) in the device which can be collected by anode (cathode), are investigated quantitatively for first time. If the current losses can be prevented, the performances of the device must be largely improved. We find that the current loss increases with the bias increasing but decreases as BR or GR increases. We also find that the $W_{\rm max}$, $J_{\rm SC}$, and FF display a stronger dependence on GR than on BR. While the $V_{\rm OC}$ values influenced by GR and BR are about the same. These results give further an insight into the mechanism and may provide a new way of improving the efficiency of BHJ solar cells.

References

[1] Li G, Zhu R and Yang Y 2012 *Nat. Photon.* **6** 153
[2] Kaltenbrunner M, White M S, Glowacki E D, Sekitani T, Someya T, Sariciftci N S and Bauer S 2012 *Nat. Commun.* **3** 770
[3] Yu G, Gao J, Hummelen J C, Wudl F and Heeger A J 1995 *Science* **270** 1789
[4] Guenes S, Neugebauer H and Sariciftci N S 2007 *Chem. Rev.* **107** 1324
[5] Thompson B C and Frechet J M J 2008 *Angew. Chem. Int. Ed.* **47** 58
[6] Brabec C J, Sariciftci N S and Hummelen J C 2001 *Adv. Funct. Mater.* **11** 15
[7] You J, Chen C C, Hong Z R, Yoshimura K, Ohya K, Xu R, Ye S, Gao J, Li G and Yang Y 2013 *Adv. Mater.* **25** 3973
[8] You J, Dou L T, Yoshimura K, Kato T, Ohya K, Moriarty T, Emery K, Chen C C, Gao J, Li G and Yang Y 2013 *Nat. Commun.* **4** 1446
[9] Xu Z X and Roy V A L 2013 *Chin. Phys. B* **22** 128505
[10] Lu C X, Yan P, Wang J Z, Liu A M, Song D and Jiang Chao 2014 *Chin. Phys. B* **23** 088803
[11] Chen W B, Yang W F, Zou H J, Tang J X, Deng L F and Li P T 2011 *Acta Phys. Sin.* **60** 117107 (in Chinese)
[12] Mandoc M M, Veurman W, Koster L J A, de Boer B and Blom P W M 2007 *Adv. Funct. Mater.* **17** 2167
[13] Mandoc M M, Kooistra F B, Hummelen J C, de Boer B and Blom P W M 2007 *Appl. Phys. Lett.* **91** 263505
[14] Proctor C M, Kim C, Neher D and Nguyen T Q 2013 *Adv. Funct. Mater.* **23** 3584
[15] Credgington D, Jamieson F C, Walker B, Nguyen T Q and Durrant J R Q 2012 *Adv. Mater.* **24** 2135
[16] Li R H, Meng W M, Peng Y Q, Ma C Z, Wang R S, Xie H W and Wang Y 2012 *Chin. Phys. Lett.* **29** 098402
[17] Koster L J A, Mihailetchi V D and Blom P W M 2006 *Appl. Phys. Lett.* **88** 052104
[18] Mihailetchi V D, Koster L J A, Hummelen J C and Blom P W M 2004 *Phys. Rev. Lett.* **93** 216601
[19] Koster L J A, Smits E C P, Mihailetchi V D and Blom P W M 2005 *Phys. Rev. B* **72** 085205
[20] Nam Y M, Huh J and Jo W H 2011 *Sol. Energy Mater. Sol. Cells* **95** 1095
[21] Monestier F, Simon J J, Torchio P, Escoubas L, Florya F, Bailly S, de Bettignies R, Guillerez S and Defranoux C 2007 *Sol. Energy Mater. Sol. Cells* **91** 405
[22] Hausermann R, Knapp E, Moos M, Reinke N A, Flatz T and Ruhstaller B 2009 *J. Appl. Phys.* **106** 104507
[23] Boland P, Lee K and Namkoong G 2010 *Sol. Energy Mater. Sol. Cells* **94** 915
[24] Koster L J A, Mihailetchi V D, Xie H and Blom P W M 2005 *Appl. Phys. Lett.* **87** 203502
[25] Koster L J A, Mihailetchi V D and Blom P W M 2006 *Appl. Phys. Lett.* **88** 093511
[26] Koster L J A, Mihailetchi V D, Ramaker R and Blom P W M 2005 *Appl. Phys. Lett.* **86** 123509
[27] Wu L L, Zang H D, and Hsiao Y C, Zhang X T and Hu B 2014 *Appl. Phys. Lett.* **104** 153903
[28] Qi B Y and Wang J Z 2013 *Phys. Chem. Chem. Phys.* **15** 8972
[29] Tumbleston J R, Ko D H, Samulski E T and Lopez R 2010 *J. Appl. Phys.* **108** 084514
[30] Zhao L, Liu D Y, Liu D M, Chen P, Zhao Y and Liu S Y 2012 *Acta Phys. Sin.* **61** 088802 (in Chinese)
[31] Yang Q Q, Zhao S L, Zhang F J, Yan G, Kong C, Fan X, Zhang Y F and Xu X R 2012 *Chin. Phys. B* **21** 128402
[32] Mihailetchi V D, Wildeman J and Blom P W M 2005 *Phys. Rev. Lett.* **94** 126602
[33] Servaites J D, Ratner M A and Marks T J 2009 *Appl. Phys. Lett.* **95** 163302